Inorganic Chemistry
Article

Inorg. Chem. **2010**, *49*, 849–859 **849**
DOI: 10.1021/ic900701s

Photocytotoxic Oxovanadium(IV) Complexes Showing Light-Induced DNA and Protein Cleavage Activity

Pijus K. Sasmal,[†] Sounik Saha,[†] Ritankar Majumdar,[‡] Rajan R. Dighe,[‡] and Akhil R. Chakravarty*,[†]

[†]*Department of Inorganic and Physical Chemistry, Indian Institute of Science, Bangalore 560012, India and* [‡]*Department of Molecular Reproduction, Development and Genetics, Indian Institute of Science, Bangalore 560012, India*

Received April 9, 2009

Oxovanadium(IV) complexes $[VO(L)(B)]Cl_2$ (**1**−**3**), where L is bis(2-benzimidazolylmethyl)amine and B is 1,10-phenanthroline (phen), dipyrido[3,2-*d*:2′,3′-*f*]quinoxaline (dpq) or dipyrido[3,2-*a*:2′,3′-*c*]phenazine (dppz), have been prepared, characterized, and their photo-induced DNA and protein cleavage activity studied. The photocytotoxicity of complex **3** has been studied using adenocarcinoma A549 cells. The phen complex **1**, structurally characterized by single-crystal X-ray crystallography, shows the presence of a vanadyl group in six-coordinate VON_5 coordination geometry. The ligands L and phen display tridentate and bidentate *N*-donor chelating binding modes, respectively. The complexes exhibit a d-d band near 740 nm in 15% DMF-Tris-HCl buffer (pH 7.2). The phen and dpq complexes display an irreversible cathodic cyclic voltammetric response near −0.8 V in 20% DMF-Tris-HCl buffer having 0.1 M KCl as supporting electrolyte. The dppz complex **3** exhibits a quasi-reversible voltammogram near −0.6 V (vs SCE) that is assignable to the V(IV)−V(III) couple. The complexes bind to calf thymus DNA giving binding constant values in the range of 6.6×10^4−2.9×10^5 M^{-1}. The binding site size, thermal melting and viscosity binding data suggest DNA surface and/or groove binding nature of the complexes. The complexes show poor "chemical nuclease" activity in dark in the presence of 3-mercaptopropionic acid or hydrogen peroxide. The dpq and dppz complexes are efficient photocleavers of plasmid DNA in UV-A light of 365 nm via a mechanistic pathway that involves formation of both singlet oxygen and hydroxyl radicals. The complexes show significant photocleavage of DNA in near-IR light (>750 nm) via hydroxyl radical pathway. Among the three complexes, the dppz complex **3** shows significant BSA and lysozyme protein cleavage activity in UV-A light of 365 nm via hydroxyl radical pathway. The dppz complex **3** also exhibits photocytotoxicity in non-small cell lung carcinoma/human lung adenocarcinoma A549 cells giving IC_{50} value of 17 μM in visible light (IC_{50} = 175 μM in dark).

Introduction

Photodynamic therapy (PDT) using porphyrin, phthalocyanine, and other organic dyes has emerged as a new modality of cancer treatment in which cancer cells are selectively targeted by light for drug-action leaving the healthy cells unaffected.[1−10] Photoactive transition metal complexes are also known to show significant photocytotoxicity in a variety of cancer cells.[11−15] The PDT drug Photofrin is a hematoporphyrin species which on photoacti-

*To whom correspondence should be addressed. E-mail: arc@ipc.iisc.ernet.in. Fax: 91-80-23600683. Phone: +91-80-22932533.

(1) Bonnett, R. *Chemical Aspects of Photodynamic Therapy*; Gordon & Breach: London, U.K., 2000.
(2) Detty, M. R.; Gibson, S. L.; Wagner, S. J. *J. Med. Chem.* **2004**, *47*, 3897.
(3) Wei, W.-H.; Wang, Z.; Mizuno, T.; Cortez, C.; Fu, L.; Sirisawad, M.; Naumovski, L.; Magda, D.; Sessler, J. L. *Dalton Trans.* **2006**, 1934.
(4) Henderson, B. W.; Busch, T. M.; Vaughan, L. A.; Frawley, N. P.; Babich, D.; Sosa, T. A.; Zollo, J. D.; Dee, A. S.; Cooper, M. T.; Bellnier, D. A.; Greco, W. R.; Oseroff, A. R. *Cancer Res.* **2000**, *60*, 525.
(5) Sternberg, E. D.; Dolphin, D.; Brückner, C. *Tetrahedron* **1998**, *54*, 4151.
(6) Ali, H.; Van Lier, J. E. *Chem. Rev.* **1999**, *99*, 2379.
(7) Rodriguez, M. E.; Moran, F.; Bonansea, A.; Monetti, M.; Fernandez, D. A.; Strassert, C. A.; Rivarola, V.; Awruch, J.; Dicelio, L. E. *Photochem. Photobiol. Sci.* **2003**, *2*, 988.
(8) Ramaiah, D.; Eckert, I.; Arun, K. T.; Weidenfeller, L.; Epe, B. *Photochem. Photobiol.* **2004**, *79*, 99.
(9) Kar, M.; Basak, A. *Chem. Rev.* **2007**, *107*, 2861.
(10) (a) Verma, S.; Watt, G. M.; Mai, Z.; Hasan, T. *Photochem. Photobiol.* **2007**, *83*, 996. (b) Atilgan, S.; Ekmeckci, Z.; Dogan, A. L.; Guc, D.; Akkaya, E. U. *Chem. Commun.* **2006**, 4398.
(11) Mackay, F. S.; Woods, J. A.; Heringová, P.; Kašpárková, J.; Pizarro, A. M.; Moggach, S. A.; Parsons, S.; Brabec, V.; Sadler, P. J. *Proc. Natl. Acad. Sci. U.S.A.* **2007**, *104*, 20743.
(12) (a) Chifotides, H. T.; Dunbar, K. R. *Acc. Chem. Res.* **2005**, *38*, 146. (b) Angeles-Boza, A. M.; Chifotides, H. T.; Aguirre, J. D.; Chouai, A.; Fu, P. K.-L.; Dunbar, K. R.; Turro, C. *J. Med. Chem.* **2006**, *49*, 6841.
(13) Mao, J.; Zhang, Y.; Zhu, J.; Zhang, C.; Guo, Z. *Chem. Commun.* **2009**, 908.
(14) Rose, M. J.; Fry, N. L.; Marlow, R.; Hinck, L.; Mascharak, P. K. *J. Am. Chem. Soc.* **2008**, *130*, 8834.
(15) Brindell, M.; Kuli, E.; Elmroth, S. K. C; Urbaska, K.; Stochel, G. *J. Med. Chem.* **2005**, *48*, 7298.

Published on Web 12/29/2009

vation of its lowest energy Q-band at 630 nm generates a $^1\pi\pi^*$ state with successive conversion to the triplet state ($^3\pi\pi^*$) that activates molecular oxygen to form cytotoxic singlet oxygen ($^1O_2$) species in a type-II pathway.[16−18] The porphyrin bases suffer from hepatotoxicity because of formation of bilirubin on oxidative conversion and skin sensitivity.[19] To circumvent the problems associated with the porphyrin bases, phthalocyanine-based organic dyes, their analogues and metal complexes are studied for their near-IR photosensitization ability.[1] Lutetium(III) texaphyrin (LUTRIN) is known to show PDT effect in near-IR light of 732 nm.[20] Unlike an organic dye that generally follows a singlet oxygen pathway, transition metal-based PDT agents are more versatile with their varied coordination geometry, tunable redox, and spectral properties that could be suitably tailored to observe photo-induced DNA cleavage activity in visible light via different mechanistic pathways.[16]

PDT agents derived from bioessential metal ions could in addition overcome the side effects and drug resistance problems associated with organic dyes and metal-based chemotherapeutic agents like cisplatin and its analogues. For example, Sadler and co-workers have reported a platinum(IV) complex $[Pt(N_3)_2(OH)_2(NH_3)(py)]$ that on photoexposure to light undergoes ligand substitutions and photoreduction of the metal to generate a cisplatin analogue which shows cytotoxic effects to cisplatin-resistant human ovarian carcinoma cells.[11] Dirhodium(II) complexes are reported to cause oxidative cellular DNA damage in visible light via both oxygen dependent and independent pathways.[12] Ruthenium(II) nitrosyl complexes are known to photocleave cellular DNA on site-specific delivery of nitric oxide (NO).[14] The reports from our laboratory have shown that copper(II) complexes having photoactive ligands like dipyridoquinoxaline (dpq) and dipyridophenazine (dppz) cleave plasmid DNA in red light.[21−25] We have shown that ternary iron(III) and binary oxovanadium(IV) complexes of dipyridophenazine (dppz) are photocytotoxic PDT agents in visible light.[26,27] Since PDT is a non-invasive method to cure cancer by causing selective photo-induced DNA damage in the cancer cells, current efforts are being directed to develop new generation PDT agents that can control both primary and secondary tumors considering the fact that the secondary tumors formed by the process of metastases are generally more fatal than the primary tumors.[28−30] The anti-metastases agents are required to target the enzymes belonging to the protein kinase family. Literature reports have shown that such enzymes can be targeted by metal complexes, namely, (η^6-arene)ruthenium(II) complexes, *trans*-tetrachlorobis(1*H*-indazole)ruthenate(III) and related species.[31−35] Designing and developing the chemistry of metal-based PDT and anti-metastasis agents thus assume considerable importance in cancer management and cure.

The present work stems from our continued interests to design new oxovanadium(IV) complexes that are capable of cleaving DNA and cellular proteins on irradiation with light. Vanadium is an essential trace element present in almost all mammalian tissue.[36] Vanadium is used as insulin mimetics and antitumor agents.[37−41] Bleomycin vanadyl(IV) and $[VO(phen)(H_2O)_2]^{2+}$ show chemical nuclease activity in the presence of H_2O_2.[42−44] Oxovanadium(V) and peroxovanadium(V) complexes are known to cleave DNA on photoexposure to UV-A light.[45−50] The vanadium(V) complexes are, however, not suitable for PDT applications in absence of any visible electronic band within the PDT spectral window. Oxovanadium(IV) complexes with a $3d^1$-electronic configuration and having low energy absorption band in the spectral window of 600−800 nm could show

(16) Szaciowski, K.; Macyk, W.; Drzewiecka-Matuszek, A.; Brindell, M.; Stochel, G. *Chem. Rev.* **2005**, *105*, 2647.
(17) Armitage, B. *Chem. Rev.* **1998**, *98*, 1171.
(18) Burrows, C. J.; Muller, J. G. *Chem. Rev.* **1998**, *98*, 1109.
(19) (a) Ochsner, M. *J. Photochem. Photobiol. B* **1996**, *32*, 3. (b) Moriwaki, S. I.; Misawa, J.; Yoshinari, Y.; Yamada, I.; Takigawa, M.; Tokura, Y. *Photodermatol., Photoimmunol. Photomed.* **2001**, *17*, 241.
(20) Young, S. W.; Woodburn, K. W.; Wright, M.; Mody, T. D.; Fan, Q.; Sessler, J. L.; Dow, W. C.; Miller, R. A. *Photochem. Photobiol.* **1996**, *63*, 892.
(21) Dhar, S.; Senapati, D.; Reddy, P. A. N.; Das, P. K.; Chakravarty, A. R. *Chem. Commun.* **2003**, 2452.
(22) Dhar, S.; Nethaji, M.; Chakravarty, A. R. *Inorg. Chem.* **2006**, *45*, 11043.
(23) Gupta, T.; Dhar, S.; Nethaji, M.; Chakravarty, A. R. *Dalton Trans.* **2004**, 1896.
(24) Patra, A. K.; Dhar, S.; Nethaji, M.; Chakravarty, A. R. *Dalton Trans.* **2005**, 896.
(25) Dhar, S.; Chakravarty, A. R. *Inorg. Chem.* **2005**, *44*, 2582.
(26) Saha, S.; Majumdar, R.; Roy, M.; Dighe, R. R.; Chakravarty, A. R. *Inorg. Chem.* **2009**, *48*, 2652.
(27) Sasmal, P. K.; Saha, S.; Majumdar, R.; Dighe, R. R.; Chakravarty, A. R. *Chem. Commun.* **2009**, 1703.
(28) Bednarski, P. J.; Mackay, F. S.; Sadler, P. J. *Anticancer Agents Med. Chem.* **2007**, *7*, 75.
(29) Hartinger, C. G.; Dyson, P. J. *Chem. Soc. Rev.* **2009**, *38*, 391.
(30) (a) Bergamo, A.; Sava, G. *Dalton Trans.* **2007**, 1267. (b) Dyson, P. J.; Sava, G. *Dalton Trans.* **2006**, 1929.
(31) (a) Liu, H.-K.; Berners-Price, S. J.; Wang, F.; Parkinson, J. A.; Xu, J.; Bella, J.; Sadler, P. J. *Angew. Chem., Int. Ed.* **2006**, *45*, 8153. (b) Yan, Y. K.; Melchart, M.; Habtemariam, A.; Sadler, P. J. *Chem. Commun.* **2005**, 4764.
(32) Pacor, S.; Zorzet, S.; Cocchietto, M.; Bacac, M.; Vadori, M.; Turrin, C.; Gava, B.; Castellarin, A.; Sava, G. *J. Pharmacol. Exp. Ther.* **2004**, *310*, 737.
(33) Sava, G.; Capozzi, I.; Clerici, K.; Gagliardi, R.; Alessio, E.; Mestroni, G. *Clin. Exp. Metastasis* **1998**, *16*, 371.
(34) Dale, L. D.; Tocher, J. H.; Dyson, T. M.; Edwards, D. I.; Tocher, D. A. *Anti-Cancer Drug Des.* **1992**, *7*, 3.
(35) Hoeschele, J. D.; Habtemariam, A.; Muir, J.; Sadler, P. J. *Dalton Trans.* **2007**, 4974.
(36) Clarke, M. J.; Zhu, F.; Frasca, D. R. *Chem. Rev.* **1999**, *99*, 2511.
(37) Crans, D. C.; Tracey, A. S. *Vanadium Compounds: Chemistry, Biochemistry, and Therapeutic Applications*; Tracey, A. S., Crans, D. C., Eds.; American Chemical Society: Washington, DC, 1998; Vol. *711*, pp 2−29.
(38) Liasko, R.; Kabanos, T. A.; Karkabounas, S.; Malamas, M.; Tasiopoulos, A. J.; Stefanou, D.; Collery, P.; Evangelou, A. *Anticancer Res.* **1998**, *18*, 3609.
(39) Evangelou, A. M. *Crit. Rev. Oncol. Hematol.* **2002**, *42*, 249.
(40) Rehder, D.; Pessoa, J. C.; Geraldes, C. F. G. C.; Castro, M. M. C. A.; Kabanos, T.; Kiss, T.; Meier, B.; Micera, G.; Pettersson, L.; Rangel, M.; Salifoglou, A.; Turel, I.; Wang, D. *J. Biol. Inorg. Chem.* **2002**, *7*, 675.
(41) Crans, D. C.; Yang, L.; Alfano, J. A.; Chi, L.-H.; Jin, W.; Mahroof-Tahir, M.; Robbins, K.; Toloue, M. M.; Chan, L. K.; Plante, A. J.; Grayson, R. Z.; Willsky, G. R. *Coord. Chem. Rev.* **2003**, *237*, 13.
(42) Kuwahara, J.; Suzuki, T.; Sugiura, Y. *Biochem. Biophys. Res. Commun.* **1985**, *129*, 368.
(43) Sakurai, H.; Tamura, H.; Okatani, K. *Biochem. Biophys. Res. Commun.* **1995**, *206*, 133.
(44) Sakurai, H.; Nakai, M.; Miki, T.; Tsuchiya, K.; Takada, J.; Matsushita, R. *Biochem. Biophys. Res. Commun.* **1992**, *189*, 1090.
(45) Hiort, C.; Goodisman, J.; Dabrowiak, J. C. *Mol. Cell. Biol.* **1995**, *153*, 31.
(46) Sam, M.; Hwang, J. H.; Chanfreau, G.; Abu-Omar, M. M. *Inorg. Chem.* **2004**, *43*, 8447.
(47) Kwong, D. W. J.; Chan, O. Y.; Shek, L. K.; Wong, R. N. S. *J. Inorg. Biochem.* **2005**, *99*, 2062.
(48) Kwong, D. W. J.; Chan, O. Y.; Wong, R. N. S.; Musser, S. M.; Vaca, L.; Chan, S. I. *Inorg. Chem.* **1997**, *36*, 1276.
(49) Hiort, C.; Goodisman, J.; Dabrowiak, J. C. *Biochemistry* **1996**, *35*, 12354.
(50) Chen, C.-T.; Lin, J.-S.; Kuo, J.-H.; Weng, S.-S.; Cuo, T.-S.; Lin, Y.-W.; Cheng, C.-C.; Huang, Y.-C.; Yu, J.-K.; Chou, P.-T. *Org. Lett.* **2004**, *6*, 4471.

Scheme 1. Ternary Structures of the VO^{2+} Complexes (**1**−**3**) and the Phenanthroline Bases Used

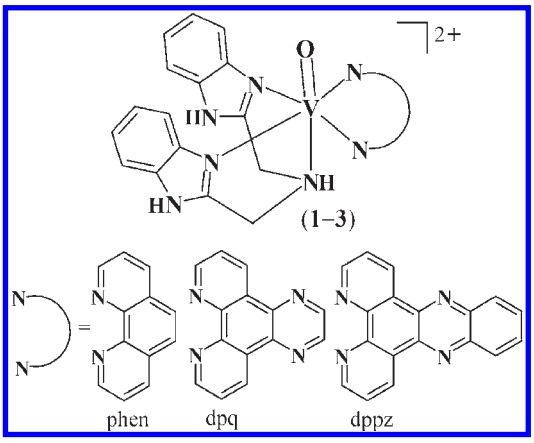

photo-induced DNA cleavage activity in near-IR light. We have chosen *N*-donor ligands since oxovanadium(IV) complexes of such ligands are expected to be redox stable in the presence of cellular thiols. This could minimize the unwanted chemical nuclease activity and cellular dark toxicity. The benzimidazole scaffold used in the present report is a useful structural motif for the development of molecules of pharmaceutical or biological interest besides controlling the metal-based redox potentials. Its derivatives have found diverse therapeutic applications as antiulcer, antiviral, antifungal, anticancer, and antihistaminic agents.[51] Benzimidazole-based various drugs like omeprazole (proton pump inhibitor), pimobendan (ionodilator), and mebendazole (anthelmintic) are known. Our recent reports have shown that Schiff base complexes of $3d^1$-vanadium(IV) having phenanthroline bases are capable of cleaving DNA on exposure to UV-A light.[52,53] The DNA cleavage activity of these Schiff base VO^{2+} complexes is, however, poor in red light. To augment the DNA cleavage activity in near-IR light, we have designed a new class of oxovanadium(IV) complexes of formulation $[VO(L)(B)]Cl_2$ (**1**−**3**), where L is bis(2-benzimidazolylmethyl)amine and B is *N,N*-donor heterocyclic base, namely, 1,10-phenanthroline (phen in **1**), dipyrido[3,2-*d*:2′,3′-*f*]quinoxaline (dpq in **2**) and dipyrido[3,2-*a*:2′,3′-*c*]phenazine (dppz in **3**) (Scheme 1). Herein, we present the synthesis, structure, DNA binding, photo-induced DNA and protein cleavage activity, and photocytotoxicity of the complexes in non-small cell lung carcinoma/human lung adenocarcinoma A549 cells. The important results include significant DNA cleavage activity of the dpq and dppz complexes in near-IR light and photocytotoxicity of the dppz complex in visible light. The dppz complex also shows photo-induced protein cleavage activity in UV-A light of 365 nm.

Experimental Section

Materials and Methods. All reagents and chemicals were procured from commercial sources (SD Fine Chemicals, India; Aldrich-Sigma, U.S.A.) and used without further purifications. Solvents used were purified by standard procedures.[54] Synthesis of the complexes was done under nitrogen atmosphere using Schlenk techniques. Supercoiled (SC) pUC19 DNA (cesium chloride purified) was purchased from Bangalore Genie (India). Tris-(hydroxymethyl)aminomethane-HCl (Tris-HCl) buffer solution was prepared using deionized and sonicated triple distilled water. Calf thymus (CT) DNA, agarose (molecular biology grade), distamycin-A, catalase, superoxide dismutase (SOD), 2,2,6,6-tetramethyl-4-piperidone (TEMP), 1,4-diazabicyclo[2.2.2]octan (DABCO), ethidium bromide (EB), Hoechst 33258 (bis-benzimidazole derivative), bovine serum albumin (BSA), lysozyme, acrylamide, *N,N*′-methylene-bis-acrylamide, ammonium persulphate, *N,N,N*′,*N*′-tetramethylethylenediamine (TEMED), 2-mercaptoethanol (MPE), tricine, glycerol, sodium dodecyl sulfate (SDS), bromophenol blue, coomassie brilliant blue R-250 were from Sigma (U.S.A.). The *N,N*-donor heterocyclic bases dipyrido[3,2-*d*:2′,3′-*f*]quinoxaline (dpq) and dipyrido[3,2-*a*:2′,3′-*c*]phenazine (dppz) were prepared by literature procedures using 1,10-phenanthroline-5,6-dione as a precursor reacted with ethylenediamine for dpq and 1,2-phenylenediamine for dppz.[55,56] Bis-(2-benzimidazolylmethyl)amine (L) was synthesized by following a reported method.[57]

The elemental analysis was done using a Thermo Finnigan Flash EA 1112 CHNS analyzer. The infrared and electronic spectra were recorded on PerkinElmer Lambda 35 and PerkinElmer Spectrum one 55 spectrophotometers, respectively. Molar conductivity measurements were performed using a Control Dynamics (India) conductivity meter. Room temperature magnetic susceptibility data were obtained from a George Associates Inc. Lewis-coil force magnetometer using $Hg[Co(NCS)_4]$ as a standard. Experimental susceptibility data were corrected for diamagnetic contributions.[58] Cyclic voltammetric measurements were made at 25 °C on a EG&G PAR Model 253 VersaStat potentiostat/galvanostat with electrochemical analysis software 270 using a three electrode setup comprising a glassy carbon working, platinum wire auxiliary, and a saturated calomel reference (SCE) electrode. Potassium chloride (KCl, 0.1 M) was used as a supporting electrolyte in DMF-water (v/v 1:5). The electrochemical data were uncorrected for junction potentials. Electrospray ionization mass spectral measurements were done using Esquire 3000 plus ESI (Bruker Daltonics) and Q-TOF Mass Spectrometer. Protein mass spectral study was done using Bruker Daltonics made Ultraflex MALDI-TOF/TOF mass spectrometer. Fluorescence microscopic investigations were carried out on Leica DM IL microscope with integrated Leica DFC400 camera and IL50 image software.

Preparation of $[VO(L)(B)]Cl_2$ (1−3) [B = phen, 1; dpq, 2; dppz, 3]. Complexes **1**−**3** were prepared by a general synthetic procedure in which vanadium(III) chloride (0.16 g, 1.0 mmol) and bis-(2-benzimidazolylmethyl)amine (L) were mixed in 20 mL of MeOH and stirred at 25 °C for 30 min. To this solution was added a methanol solution (10 mL) of the heterocyclic base (1.0 mmol: 0.2 g, phen; 0.23 g, dpq; 0.29 g, dppz). The resulting mixture was stirred for an hour to obtain a brown solution that was kept for evaporation of the solvent. A green solid thus obtained was isolated, washed with Et_2O, and finally dried in vacuum over P_4O_{10} [Yield: ∼75%]. Anal. Calcd for $C_{28}H_{23}N_7OCl_2V$ (**1**): C, 56.49; H, 3.89; N, 16.47. Found: C, 56.32; H, 3.82; N, 16.35. ESI-MS in MeOH: *m*/*z* 523 $[M-2Cl-H]^+$.[59]

(51) Spasov, A. A.; Yozhitsa, I. N.; Bugaeva, L. I.; Anisimova, V. A. *Pharm. Chem. J.* **1999**, *33*, 232.
(52) Sasmal, P. K; Patra, A. K; Nethaji, M; Chakravarty, A. R. *Inorg. Chem.* **2007**, *46*, 11112.
(53) Sasmal, P. K.; Patra, A. K.; Chakravarty, A. R. *J. Inorg. Biochem.* **2008**, *102*, 1463.
(54) Perrin, D. D.; Armarego, W. L. F.; Perrin, D. R. *Purification of Laboratory Chemicals*; Pergamon Press: Oxford, 1980.
(55) Collins, J. G.; Sleeman, A. D.; Aldrich-Wright, J. R.; Greguric, I.; Hambley, T. W. *Inorg. Chem.* **1998**, *37*, 3133.
(56) (a) Dickeson, J. E.; Summers, L. A. *Aust. J. Chem.* **1970**, *23*, 1023. (b) Amouyal, E.; Homsi, A.; Chambron, J.-C.; Sauvage, J.-P. *J. Chem. Soc., Dalton Trans.* **1990**, 1841.
(57) Berends, H. P.; Stephan, D. W. *Inorg. Chim. Acta* **1984**, *93*, 173.
(58) Kahn, O. *Molecular Magnetism*, VCH: Weinheim, Germany, 1993.
(59) Zhang, G.-Q; Yang, G.-Q; Yang, L.-Y; Chen, Q.-Q; Ma, J.-S. *Eur. J. Inorg. Chem.* **2005**, 1919.

Λ_M = 189 S m^2 M^{-1} in 15% DMF-H_2O at 25 °C. Selected IR data (KBr phase, cm^{-1}): 3397 br, 2910 w, 1624 m, 1521 m, 1475 m, 1454 m, 1428 m, 1280 m, 1221w, 1055 m, 982 s (V=O), 851 m, 749 s (br, broad; s, strong; m, medium; w, weak). UV−visible in 15% DMF-Tris-HCl buffer [λ_{max}/nm (ε/ M^{-1} cm^{-1})]: 740 (40), 521sh (50), 438sh (90), 279 (19580), 273 (20750) (sh, shoulder). μ_{eff} = 1.66 μ_B at 298 K. Anal. Calcd for $C_{30}H_{23}N_9OCl_2V$ (**2**): C, 55.66; H, 3.58; N, 19.47. Found: C, 55.52; H, 3.52; N, 19.45. ESI-MS in MeOH: m/z 575 [M−2Cl−H]$^+$.[59] Λ_M = 185 S m^2 M^{-1} in 15% DMF-H_2O at 25 °C. Selected IR data (KBr phase, cm^{-1}): 3407 br, 3106 w, 1621 m, 1487 m, 1450 m, 1278 m, 1218 m, 1053 w, 984 s (V=O), 901 m, 820 w, 759 s. UV−visible in 15% DMF-Tris-HCl buffer [λ_{max}/nm (ε/M^{-1} cm^{-1})]: 738 (55), 523sh (80), 436sh (180), 341 (3170), 326 (4970), 272 (25600), 254 (23680). μ_{eff} = 1.63 μ_B at 298 K. Anal. Calcd for $C_{34}H_{25}N_9OCl_2V$ (**3**): C, 58.55; H, 3.61; N, 18.07. Found: C, 58.52; H, 3.65; N, 18.01. ESI-MS in MeCN: m/z 625 [M−2Cl−H]$^+$.[59] Λ_M = 182 S m^2 M^{-1} in 15% DMF-H_2O at 25 °C. Selected IR data (KBr phase, cm^{-1}): 3063 br, 2921 w, 1626 m, 1496 m, 1459 m, 1276 m, 1221 m, 1052 w, 983 s (V=O), 903 m, 750 s. UV−visible in 15% DMF-Tris-HCl buffer [λ_{max}/nm (ε/ M^{-1} cm^{-1})]: 735 (65), 537sh (160), 426sh (670), 380 (3200), 362 (3380), 279 (22460), 273 (23680). μ_{eff} = 1.62 μ_B at 298 K.

Solubility and Stability. The complexes were soluble in DMF and DMSO, moderately soluble in H_2O and MeOH, less soluble in MeCN and CH_2Cl_2, and insoluble in hydrocarbon solvents. They were stable in the solid and solution phases.

X-ray Crystallographic Procedure. The crystal structure of **1** was obtained by a single crystal X-ray diffraction technique. The complex was crystallized from its methanol solution on slow evaporation of the solvent. Crystal mounting was done on glass fiber with epoxy cement. All geometric and intensity data were collected at room temperature using an automated Bruker SMART APEX CCD diffractometer equipped with a fine focus 1.75 kW sealed tube Mo Kα X-ray source (λ = 0.71073 Å) with increasing ω (width of 0.3° per frame) at a scan speed of 2 s per frame. Intensity data, collected using an ω-2θ scan mode, were corrected for Lorentz−polarization effects and for absorption.[60] Structure was solved by the combination of Patterson and Fourier techniques and refined by full-matrix least-squares method using the SHELX system of programs.[61] Hydrogen atoms belonging to the complex were in their calculated positions and refined using a riding model. All non-hydrogen atoms were refined anisotropically. Selected crystallographic data are given in Table 1. A perspective view of the complex was obtained with the Oak Ridge Thermal Ellipsoid Plot Program (ORTEP).[62]

DNA Binding Methods. The experiments were done using the complex solution in Tris-HCl buffer (5 mM Tris-HCl, pH 7.2) containing DMF (15%). Calf thymus (CT) DNA (ca. 350 μM NP) in this buffer medium gave a ratio of UV absorbance at 260 and 280 nm of about 1.9:1 indicating the DNA apparently free from protein impurity. The concentration of CT DNA was estimated from its absorption band intensity at 260 nm with a known molar extinction coefficient value (ε) of 6600 M^{-1} cm^{-1}.[63] Absorption titration experiments were carried out by varying the concentration of the CT DNA while keeping the oxovanadium(IV) complex concentration as constant. Due correction was made for the absorbance of CT DNA itself. Each spectrum was recorded after equilibration for 5 min. The intrinsic equilibrium binding constant (K_b) and the binding site size (s) of the complexes **1**−**3** to CT DNA were obtained by the McGhee−von Hippel (MvH) method using the expression of Bard and co-workers by monitoring the change in the absorption intensity of the spectral bands with increasing concentration of CT DNA by regression analysis using equation: $(\varepsilon_a - \varepsilon_f)/(\varepsilon_b - \varepsilon_f) = (b - (b^2 - 2K_b^2C_t[DNA]_t/s)^{1/2})/2K_bC_t$, where $b = 1 + K_bC_t + K_b[DNA]_t/2s$, ε_a is the extinction coefficient observed for the absorption band at a given DNA concentration, ε_f is the extinction coefficient of the complex free in solution, ε_b is the extinction coefficient of the complex when fully bound to DNA, K_b is the equilibrium binding constant, C_t is the total metal complex concentration, $[DNA]_t$ is the DNA concentration in nucleotides, and s is the binding site size in base pairs.[64,65] The non-linear least-squares analysis was done using Origin Lab, version 6.1.

DNA melting experiments were done by monitoring the absorption intensity of CT DNA (170 μM) at 260 nm at various temperatures, both in the absence and in the presence of the oxovanadium(IV) complexes (10 μM). Measurements were carried out using a Cary 300 bio UV−visible spectrometer attached to a Cary temperature controller on increasing the temperature of the solution by 0.5 °C per min. Viscometric titrations were performed with a Schott Gerate AVS 310 Automated Viscometer. The viscometer was thermostatted at 37 °C in a constant temperature bath. The initial concentration of CT DNA was 140 μM in NP (nucleotide pair), and the flow times were measured with an automated timer. Each reading was taken on addition of 100 μL of complex stock solution of 1 mM. Each sample was measured 3 times, and an average flow time was calculated. Data were presented as $(\eta/\eta_0)^{1/3}$ versus [complex]/[DNA], where η is the viscosity of DNA in the presence of the complex and η_0 is that of DNA alone. Viscosity values were calculated from the observed flow time of DNA-containing solutions (t) corrected for that of the buffer alone (t_0), $\eta = (t - t_0)/t_0$.

DNA Cleavage Experiments. The cleavage of supercoiled (SC) pUC19 DNA (30 μM, 0.2 μg, 2686 base-pairs) was studied by agarose gel electrophoresis using metal complexes in 50 mM Tris-HCl buffer (pH 7.2) containing 50 mM NaCl and 1.5% DMF. For photo-induced DNA cleavage studies, the reactions

Table 1. Selected Crystallographic Data for [VO(L)(phen)]$Cl_2 \cdot 4H_2O$ (**1**·$4H_2O$)

formula	$C_{28}H_{31}N_7O_5Cl_2V$
crystal size (mm^3)	0.35 × 0.27 × 0.21
Fw, g M^{-1}	667.44
crystal system	triclinic
space group (no.)	$P\bar{1}$ (2)
a, Å	10.411(4)
b, Å	12.732(5)
c, Å	12.961(5)
α, deg	113.664(6)
β, deg	93.486(7)
γ, deg	90.775(7)
V, Å^3	1569.4(10)
Z	2
T, K	293(2)
density (calc) (g cm^{-3})	1.412
λ, Å (Mo-K$_\alpha$)	0.71073
μ (mm^{-1})	0.535
data/restraints/parameters	5512/0/388
goodness-of-fit on F^2	0.972
$R(F_o)^a$ [$I > 2\sigma(I)$]	0.1083
$wR(F_o)^b$ [$I > 2\sigma(I)$]	0.2656
R [all data] (wR [all data])	0.2124 (0.3309)
largest diff. peak and hole (e Å^{-3})	0.768, −0.866

$^a R = \sum||F_o| - |F_c||/\sum|F_o|$. $^b wR = \{\sum w(F_o^2 - F_c^2)^2/\sum w(F_o^2)\}^{1/2}$; $w = [\sigma^2(F_o)^2 + (AP)^2 + BP]^{-1}$, where $P = (F_o^2 + 2F_c^2)/3$; A and B values are 0.1816 and 1.0894, respectively.

(60) Walker, N.; Stuart, D. *Acta Crystallogr.* **1993**, *A39*, 158.
(61) Sheldrick, G. M. *SHELX-97, Programs for Crystal Structure Solution and Refinement*; University of Göttingen: Göttingen, Germany, 1997.
(62) Johnson, C. K. *ORTEP, Report ORNL-5138*; Oak Ridge National Laboratory: Oak Ridge, TN, 1976.
(63) Reichmann, M. E.; Rice, S. A.; Thomas, C. A.; Doty, P. *J. Am. Chem. Soc.* **1954**, *76*, 3047.
(64) McGhee, J. D.; von Hippel, P. H. *J. Mol. Biol.* **1974**, *86*, 469.
(65) Carter, M. T.; Rodriguez, M.; Bard, A. J. *J. Am. Chem. Soc.* **1989**, *111*, 8901.

were carried out under illuminated conditions using UV-A light of 365 nm (6 W, Model LF-206.LS) or near IR light of > 750 nm using a Spectra Physics Water-Cooled Mixed-Gas Ion Laser Stabilite 2018-RM (continuous-wave (CW) beam diameter at $1/e^2$ of 1.8 mm ± 10% and beam divergence with full angle of 0.7 mrad ± 10%) with an attachment Model 2018-RM-IR having all-lines IR optics (752.5−799.3 nm). The laser beam power at the sample position (5 cm from the aperture with a solution path length of 5 mm) was 100 mW, measured using Spectra Physics CW Laser Power Meter (Model 407A). After light exposure, each sample was incubated for 1.0 h at 37 °C and analyzed for the photo-cleaved products using gel electrophoresis. The mechanistic studies were carried out using different additives (NaN_3, 0.2 mM; TEMP, 0.2 mM; DABCO, 0.2 mM; DMSO, 4 μL; KI, 0.2 mM; catalase, 4 units; SOD, 4 units) prior to the addition of the complex. For the D_2O experiment, this solvent was used for dilution of the sample to 20 μL final volume. The samples after incubation in a dark chamber were added to the loading buffer containing 0.25% bromophenol blue, 0.25% xylene cyanol, 30% glycerol (3 μL) and the solution was finally loaded on 1% agarose gel containing 1.0 μg/mL ethidium bromide. Electrophoresis was carried out in a dark room for 2.0 h at 60 V in TAE (Tris-acetate EDTA) buffer. Bands were visualized by UV light and photographed. The extent of SC DNA cleavage was measured from the intensities of the bands using UVITEC Gel Documentation System. Due corrections were made for the low level of nicked circular (NC) form of DNA present in the original SC DNA sample and for the low affinity of EB binding to SC compared to NC and linear forms of DNA.[66] The concentrations of the complexes and additives corresponded to that in the 20 μL of final volume of the sample using Tris buffer. The observed error in measuring the band intensities was ∼5%.

Protein Cleavage Experiments. Photo-induced protein cleavage experiments were carried out following the literature procedure described by Kumar and co-workers.[67] Freshly prepared solutions of BSA and lysozyme in 50 mM Tris-HCl buffer (pH 7.2) containing 1.8% DMF were used for the photochemical protein cleavage studies. The protein solutions in Tris-HCl buffer medium containing complexes **1**−**3** having concentrations of 100 and 125 μM for BSA (5 μM) and 50 and 100 μM for lysozyme (10 μM) were photo-irradiated at 365 nm (100 W) for 1.0 h in Eppendorf vials. The BSA and lysozyme solutions in the presence of the complexes were incubated at 37 °C for 1.0 h prior to the photoexposure. The photo-irradiated samples (50 μL) were dried in an EYELA Centrifugal Vaporizer (Model CVE-200D), and the samples were dissolved in the loading buffer (24 μL) containing SDS (7% w/v), glycerol (4% w/v), Tris-HCl buffer (50 mM, pH 6.8), mercaptoethanol (2% v/v), and bromophenol blue (0.01% w/v). The protein solutions were then denatured on heating to boil for 3 min. The samples were loaded on a 3% polyacrylamide stacking gel. The gel electrophoresis was done at 60 V until the dye passed into the separating gel from the stacking (3%) gel, and then the voltage was increased to 120 V. The gels were run for 1.5 h, stained with Coomassie Brilliant Blue R-250 solution (acetic acid/methanol/water = 1:2:7 v/v) and destained with water/methanol/acetic acid mixture (5:4:1 v/v) for 4 h. The gels, after destaining, were scanned with a HP Scanjet G3010 scanner, and the images were further processed using Adobe Photoshop 7.0 software package. Molecular weight markers were used in each gel to calibrate the molecular weight of the protein. The presence of reactive oxygen species was investigated by carrying out the photo-induced protein cleavage experiments in the presence of singlet oxygen quenchers like NaN_3 (3 mM) and TEMP (3 mM) and hydroxyl radical scavengers like DMSO (20 μL) and KI (3 mM). For lysozyme, 16.5%/4% tricine SDS-PAGE was performed after photoexposure following a reported method.[68]

Cell Cytotoxicity Assay. The photocytotoxicity of the dppz complex **3** was studied using 3-(4,5-dimethylthiazol-2-yl)-2,5-diphenyltetrazolium bromide (MTT) assay which is based on the ability of mitochondrial dehydrogenases of viable cells to cleave the tetrazolium rings of MTT forming dark purple membrane impermeable crystals of formazan that could be quantified at 595 nm in DMSO.[69] Approximately, 8000 cells of human lung adenocarcinoma (A549) were plated in 96 wells culture plate in Dulbecco's Modified Eagle Medium (DMEM) containing 10% FBS and after 24 h of incubation at 37 °C in CO_2 incubator, various concentrations of complex **3** dissolved in 1% DMSO were added to the cells and incubation was continued for 3 h in dark. The medium was subsequently replaced with PBS and photo-irradiated with visible light (400−700 nm) using a Luzchem Photoreactor (Model LZC-1, Ontario, Canada) fitted with Sylvania fluorescent white tubes with a fluence rate of 2.4 mW cm^{-2} to provide a total dose of 10 J cm^{-2}. After photoexposure, PBS was removed and replaced with DMEM-FBS, and incubation was continued for further 12 h in dark. At the end of the incubation period, 20 μL of 5 mg mL^{-1} of MTT was added to each well and incubated for an additional 3 h. The culture medium was finally discarded, 200 μL of DMSO was added to dissolve the formazan crystals, and the absorbance at 595 nm was determined using a BIORAD ELISA plate reader. Cytotoxicity of complex **3** was measured as the percentage ratio of the absorbance of the treated cells to the untreated controls. The IC_{50} values were determined by non-linear regression analysis (GraphPad Prism).

Nuclear Staining. This was performed by following reported procedures.[70] Briefly, the cells after photo-exposure with visible light (400−700 nm, 10 J cm^{-2}) for 4 h were washed with PBS and fixed in 3.7% paraformaldehyde for 10 min. The fixed cells were then permeabilized with TBST [50 mM Tris-HCl (pH 7.4), 150 mM NaCl, and 0.1% Triton X-100] for 5 min. Cells were washed with PBS and then a 4′,6-diamidino-2-phenylindole (DAPI) solution (10 μg mL^{-1} in PBS) was added to the cells and kept for 5 min. After several washings with PBS, the cells were observed under a fluorescence microscope (Leica DM IL microscope with integrated Leica DFC 320 R2 camera and IL50 image software) with 360/40 nm excitation and 460/50 nm emission filters to ascertain any condensation or fragmentation of the nuclei indicating cells undergoing apoptosis.

Results and Discussion

Synthesis and General Aspects. Oxovanadium(IV) complexes $[VO(L)(B)]Cl_2$ (**1**−**3**), where L is bis-(2-benzimidazolylmethyl)amine and B is phen, dpq, or dppz, have been prepared from a general synthetic procedure in which vanadium(III) chloride is reacted with L and the heterocyclic base in methanol (Scheme 1). The complexes have been characterized from the analytical and mass spectral data (Figures S1−S3 in the Supporting Information). Selected physicochemical data for the complexes are given in Table 2. The complexes are 1:2 electrolytic giving molar conductivity values of ∼185 S m^2 M^{-1} in 15% DMF-H_2O at 25 °C. The effective magnetic moment values of the complexes are of ∼1.62 μ_B indicating one-electron paramagnetic nature of the complexes. The complexes show characteristic vanadyl (V=O) infrared band at ∼980 cm^{-1}.

(66) Bernadou, J.; Pratviel, G.; Bennis, F.; Girardet, M.; Meunier, B. *Biochemistry* **1989**, *28*, 7268.
(67) Kumar, C. V.; Buranaprapuk, A.; Sze, H. C.; Jockusch, S.; Turro, N. J. *Proc. Natl. Acad. Sci. U.S.A.* **2002**, *99*, 5810.
(68) Schägger, H; Jagow, G. V. *Anal. Biochem.* **1987**, *166*, 368.
(69) Mosmann, T. *J. Immunol. Methods* **1983**, *65*, 55.
(70) Park, S.; Hong, S. P.; Oh, T. Y.; Bang, S.; Chung, J. B.; Song, S. Y. *Photochem. Photobiol. Sci.* **2008**, *7*, 769.

Table 2. Physicochemical Data for the Complexes **1**−**3**

complex	[VO(L)(phen)]Cl_2 (**1**)	[VO(L)(dpq)]Cl_2 (**2**)	[VO(L)(dppz)]Cl_2 (**3**)
IR[a], $cm^{-1}\nu$ (V=O)	982	984	983
λ, nm (ε, M^{-1} cm^{-1})[b]	740 (40)	738 (55)	735 (65)
μ_{eff}[c]	1.66	1.63	1.62
Λ_M[d] /S m^2 M^{-1}	189	185	182
$E_{1/2}$, V [ΔE_p, mV][e]	−0.88[f]	−0.78[f]	−0.56 [190]
K_b/ M^{-1} [*s*][g]	6.6(±0.4) × 10^4 [0.1]	1.2(±0.3) × 10^5 [0.2]	2.9(±0.6) × 10^5 [0.4]
ΔT_m[h]/°C	1.20	1.91	2.66

[a] In KBr phase. [b] Visible electronic band in 15% DMF-Tris-HCl buffer. [c] μ_{eff} in μ_B for solid powdered samples at 298 K. [d] Λ_M, molar conductance in 15% DMF-H_2O at 25 °C. [e] Cyclic voltammogram in 20% DMF-Tris-HCl buffer having 0.1 M KCl as supporting electrolyte at 50 mV s^{-1} scan rate. [f] Cathodic peak potential without showing any anodic counterpart. [g] K_b, DNA binding constant (*s*, binding site size). K_b values of $VOSO_4$, L, dpq and dppz are 2.3 × 10^3, 4.1 × 10^3, 3.2 × 10^4, and 7.2 × 10^4 M^{-1}, respectively. [h] Change in the DNA melting temperature.

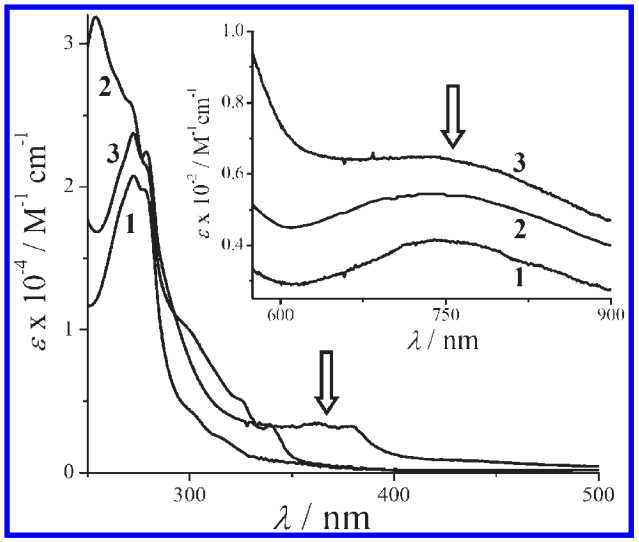

Figure 1. Electronic absorption spectra of the complexes **1**−**3** in 15% DMF-Tris-HCl buffer (wavelengths 365 and 750 nm used for DNA photocleavage experiments are shown by arrow).

The oxovanadium(IV) complexes exhibit a d-d band near 740 nm in 15% DMF-Tris HCl buffer with molar extinction coefficient values ranging within 40−65 M^{-1} cm^{-1} (Figure 1). An additional metal-centered band is observed near 430 nm. All the complexes display ligand centered bands at ∼278 and ∼270 nm. The dpq and dppz ligands with their respective quinoxaline and phenazine moiety exhibit an additional band near 350 nm assignable to the n → π^* transition.[71]

Electrochemistry. Complexes **1**−**3** are redox active showing cyclic voltammetric (CV) responses involving the metal center and the ligands in 20% DMF-Tris-HCl buffer−0.1 M KCl (Table 2, Figure S4 in the Supporting Information). The phen and dpq complexes display an irreversible voltammetric response showing the cathodic peak at −0.9 and −0.8 V, respectively, without having any anodic counterpart. This redox process is assignable to the V(IV)/V(III) couple.[72] A quasi-reversible CV response is observed for the dppz complex **3** at −0.56 V with a peak-to-peak (ΔE_p) separation of 190 mV at a scan rate of 50 mV s^{-1}. The redox process is assignable to the V(IV)−V(III) couple. In addition, one broad anodic response (E_{pa}) is observed near 1.5 V. The redox data are of importance since the complexes are expected to show poor "chemical nuclease" activity in absence of any cyclic voltammetric response within the voltage window of +1.5 to −0.6 V. All the complexes show ligand-based reductions. The phen complex shows one irreversible ligand reduction peak near −1.5 V. The dpq and dppz complexes display two redox processes. The first ligand-reduction has been observed for the dpq and dppz ligand near −1.1 and −0.92 V, respectively. The second reductive process is observed near −1.5 and −1.4 V for respective dpq and dppz ligand.

Table 3. Selected Bond Distances (Å) and Angles (deg.) for [VO(L)(phen)]Cl_2 (**1**·$4H_2O$) with e.s.d.s in the Parentheses

V(1)−O(1)	1.570(6)	N(1)−V(1)−N(2)	77.8(3)
V(1)−N(1)	2.111(7)	N(1)−V(1)−N(3)	90.3(3)
V(1)−N(2)	2.123(7)	N(1)−V(1)−N(5)	84.4(3)
V(1)−N(3)	2.064(7)	N(1)−V(1)−N(6)	158.1(3)
V(1)−N(5)	2.372(7)	N(2)−V(1)−N(3)	156.5(3)
V(1)−N(6)	2.079(7)	N(2)−V(1)−N(5)	83.8(3)
O(1)−V(1)−N(1)	102.7(3)	N(2)−V(1)−N(6)	93.1(3)
O(1)−V(1)−N(2)	102.6(3)	N(3)−V(1)−N(5)	74.8(3)
O(1)−V(1)−N(3)	99.7(3)	N(3)−V(1)−N(6)	90.6(3)
O(1)−V(1)−N(5)	171.1(3)	N(5)−V(1)−N(6)	74.7(3)
O(1)−V(1)−N(6)	98.7(3)		

Crystal Structure. The phen complex (**1**·$4H_2O$) has been structurally characterized by single-crystal X-ray diffraction technique. Selected bond distances and angles are given in Table 3. An ORTEP view of the complex is shown in Figure 2 (Figure S5 in the Supporting Information). The crystal structure shows the complex as a dicationic monomeric vanadium(IV) species with a VO^{2+} moiety bonded to a tridentate bis-(2-benzimidazolylmethyl)amine ligand (L) and a *N,N*-donor 1,10-phenanthroline (phen) base. There are two lattice chloride ions showing chemically significant hydrogen bonding interactions. The ligand L is bound to the metal through three nitrogen atoms with the amine nitrogen at the *trans* position to the vanadyl group. The lattice water molecules in **1**·$4H_2O$ are involved in intermolecular bifurcated H-bonding interactions with the nitrogen atoms of the imidazolyl moieties and the chloride anion giving distances in the range of 2.75−3.05 Å. The chloride ions are also involved in weak H-bonding interactions with imidazolyl nitrogen atoms giving a distance of 3.18 Å. The V=O distance in the $V^{IV}ON_5$ coordination geometry is 1.570(6) Å. The V−N bond *trans* to the V=O group is significantly long compared to the other V−N distances. The V−N (L) distances are shorter than the V−N (phen) distances. The V−N(sp^3) bond of 2.372(7) Å

(71) Toshima, K.; Takano, R.; Ozawa, T.; Matsumura, S. *Chem. Commun.* **2002**, 212.

(72) (a) Cooper, S. R.; Koh, Y. B.; Raymond, K. N. *J. Am. Chem. Soc.* **1982**, *104*, 5092. (b) Mahroof- Tahir, M.; Keramidas, A. D.; Goldfarb, R. B.; Anderson, O. P.; Miller, M. M.; Crans, D. C. *Inorg. Chem.* **1997**, *36*, 1657.

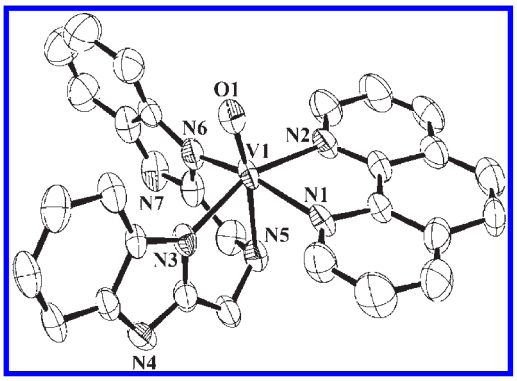

Figure 2. ORTEP view of $[VO(L)(phen)]Cl_2$ (**1**) showing atom labeling for the metal and heteroatoms and 50% probability thermal ellipsoids. The hydrogen atoms are not shown for clarity.

is significantly longer than the V−N(sp^2) bond lengths ranging within 2.064 to 2.123 Å. Although V−N(sp^3) bonds are generally known to be longer than V−N(sp^2) bonds, the *trans* effect possibly has led to the considerable lengthening of the V−N(sp^3) bond.[73]

DNA Binding. Absorption titration technique has been used to monitor the interaction of the complexes **1**−**3** with CT DNA (Table 2, Figure S6 in the Supporting Information). We have observed that binding of a complex to DNA generally leads to hypochromism along with a bathochromic shift of the electronic spectral bands resulting from strong stacking interaction between the aromatic chromophore of the ligand in the complex and the base pairs of DNA. The extent of hypochromism gives a measure of the strength of DNA binding. The trend in hypochromism among the present complexes follows the order: **3** (dppz) > **2** (dpq) > **1** (phen). The intrinsic equilibrium DNA binding constants (K_b) of the complexes along with the binding site size (s) are given in Table 2. The dppz complex shows higher K_b value in comparison to the dpq and phen analogues possibly because of the presence of an extended aromatic moiety in dppz.[74] We have done DNA binding experiments using ethidium bromide as a DNA intercalator, 4′,6-diamidino-2-phenylindole (DAPI) as DNA groove binder, and $[Cu(bpy)_2(H_2O)](ClO_4)_2$ as DNA surface binder, and the results are compared with those of **1**−**3** (Figure S7 in the Supporting Information). It is evident from the data that complexes **1** and **2** have surface or groove binding propensity, while complex **3** is a partial DNA intercalator. The binding propensities of the metal salt and the ligands to CT DNA are also measured. The dpq and dppz ligands alone show significant DNA binding affinity giving K_b values of $\sim 10^4$ M^{-1} (Table 2, Figure S7 in the Supporting Information).

Thermal denaturation and viscosity measurements have been done to explore the binding of the complexes **1**−**3** to CT DNA (Table 2, Figure 3(a)). A small positive shift of DNA melting temperature (ΔT_m) is observed on addition of the complexes to CT DNA. The low ΔT_m values for **1**−**3** suggest primarily groove binding of the

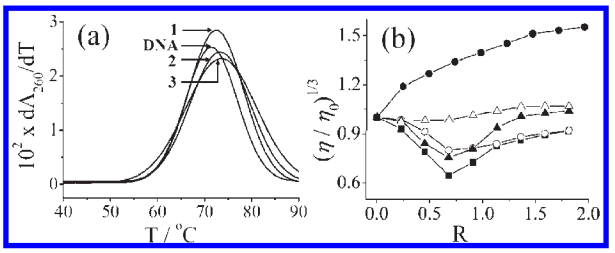

Figure 3. (a) Thermal denaturation plots of 170 μM CT DNA alone and in the presence of the complexes **1**−**3** (10 μM). (b) Effect of increasing the concentration of the complexes **1** (■), **2** (○), **3** (▲), EB (●), and Hoechst 33258 (Δ) on the relative viscosities of CT-DNA at 37.0 (±0.1) °C, R = [compound]/[DNA]). The ligand to base pair ratios (R) used for the measurements are 0.227, 0.454, 0.680, 0.907, 1.134, 1.360, 1.587, and 1.814.

complexes to CT DNA stabilizing the DNA double helix structure in preference to an intercalative mode of binding to DNA that normally gives a large positive ΔT_m value.[75,76] Viscosity measurements have been carried out to examine the effect of the vanadyl complexes on the specific relative viscosity of DNA (Figure 3(b), Figure S8 in the Supporting Information). Since the relative specific viscosity (η/η_0) of DNA gives a measure on the increase in contour length associated with the separation of DNA base pairs caused by intercalation, a classical DNA intercalating species like EB shows a significant increase in the viscosity of the DNA solutions (η and η_0 are the specific viscosities of DNA in the presence and absence of the complexes, respectively). In contrast, a partial and/or non-intercalation of the complex could result in less pronounced effect on the viscosity.[77] It is observed that DNA groove binder Hoechst 33258 shows no significant change in the DNA viscosity suggesting no effective change in the length of DNA helix. The plot of relative specific viscosity $(\eta/\eta_0)^{1/3}$ versus [complex]/[DNA] ratio shows first a decrease in the viscosity with subsequent increase leading to saturation. The viscosity data indicate partial or non-classical intercalative DNA binding mode of the complexes. The low [complex]/[DNA] ratio leads to a decrease in hydrodynamic DNA length possibly because of introduction of kinks in the DNA helix thus resulting initial decrease in viscosity.[78] At higher binding ratio, more such kinks could lead to rod-like DNA structure that increases the DNA viscosity as observed by Chaires and co-workers for tris(phenanthroline)-ruthenium(II) enantiomers.[78]

Chemical Nuclease Activity. We have studied the cleavage of supercoiled (SC) pUC19 DNA (0.2 μg, 30 μM) by the complexes **1**−**3** (50 μM) in Tris-HCl/NaCl medium containing 1.5% DMF in dark using 3-mercaptopropionic acid (MPA, 0.2 mM) as a reducing agent and hydrogen peroxide (0.2 mM) as an oxidizing agent. The complexes are found to show poor chemical nuclease activity. The cleavage of SC DNA to its nicked circular (NC) form has been observed only at high complex concentration in the presence of both MPA and hydrogen peroxide (Figures S9, S10 in the Supporting Information).

(73) Young, M. J.; Wahnon, D.; Hynes, R. C.; Chin, J. *J. Am. Chem. Soc.* **1995**, *117*, 9441.
(74) (a) Erkkila, K. E.; Odom, D. T.; Barton, J. K. *Chem. Rev.* **1999**, *99*, 2777. (b) Delaney, S.; Pascaly, M.; Bhattacharya, P. K.; Han, K.; Barton, J. K. *Inorg. Chem.* **2002**, *41*, 1966.
(75) An, Y.; Liu, S.-D.; Deng, S.-Y.; Ji, L.-N.; Mao, Z.-W. *J. Inorg. Biochem.* **2006**, *100*, 1586.
(76) Eichhorn, G. L.; Shin, Y. A. *J. Am. Chem. Soc.* **1968**, *90*, 7323.
(77) Veal, J. M.; Rill, R. L. *Biochemistry* **1991**, *30*, 1132.
(78) Satyanarayana, S.; Dabrowiak, J. C.; Chaires, J. B. *Biochemistry* **1993**, *32*, 2573.

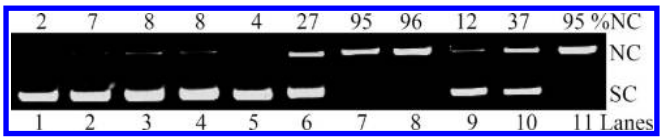

Figure 4. Cleavage of SC pUC19 DNA (0.2 μg, 30 μM) by the complexes **1**−**3** (10 μM) in 50 mM Tris-HCl/NaCl buffer (pH, 7.2) containing 1.5% DMF on photo-irradiation at 365 nm (6 W) for 1 h exposure time: lane 1, DNA control; lane 2, DNA + dpq (10 μM); lane 3, DNA + dppz (10 μM); lane 4, DNA + L (10 μM); lane 5, DNA + **3** (in dark), lanes 6−8, DNA + complexes **1**−**3**; lane 9, DNA + distamycin-A (50 μM); lane 10, DNA + distamycin-A (50 μM) + **2**; lane 11, DNA + distamycin-A (50 μM) + **3**.

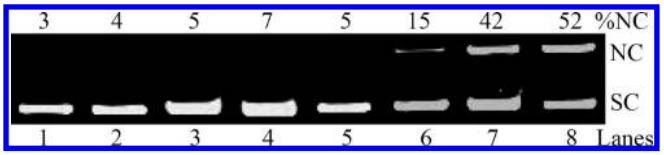

Figure 5. Cleavage of SC pUC19 DNA (0.2 μg, 30 μM) by the complexes **1**−**3** (45 μM) in 50 mM Tris-HCl/NaCl buffer (pH, 7.2) containing 1.5% DMF in red light of $\lambda > 750$ nm (100 mW) with an exposure time of 2 h: lane 1, DNA control; lane 2, DNA + dpq; lane 3, DNA + dppz; lane 4, DNA + L; lane 5, DNA + **3** (in dark); lanes 6−8, DNA + complexes **1**−**3**.

The complexes do not show any DNA cleavage activity in dark in absence of any external reagent thus excluding the possibility of any hydrolytic cleavage of DNA. The mechanistic study on the complexes has been carried out using several additives. Additions of singlet oxygen quenchers like NaN_3 and TEMP do not show any apparent effect on the DNA cleavage activity. Hydroxyl radical scavengers like DMSO, KI and catalase show significant inhibition in the DNA cleavage activity. The results suggest the involvement of hydroxyl radicals as the cleavage active species. While the present complexes show poor chemical nuclease activity, oxo-bridged divanadium(III) complexes having 1,10-phenanthroline ligand are known to cleave plasmid DNA by the formation of hydroxyl or superoxide radicals.[79] Bleomycin-vanadyl(IV) and $VO(phen)^{2+}$ complexes cleave DNA in an oxidative manner in the presence of hydrogen peroxide.[42−45] The poor chemical nuclease activity of the present complexes could be due to their redox stability within the voltage window of +1.0 to −0.6 V (vs SCE).

Photonuclease Activity. The photo-induced DNA cleavage activity of the complexes has been studied using SC pUC19 DNA in Tris-HCl/NaCl buffer containing 1.5% DMF on irradiation with monochromatic UV-A light of 365 nm and red light of >750 nm (Figures 4 and 5, Figures S11 and S12 in the Supporting Information). The phen complex **1**, in absence of any photoactive ligand moiety, is a poor cleaver of DNA in UV-A light (Figure 4, lane 6). A 10 μM solution of the dpq and dppz complexes **2** and **3** on photo-irradiation at 365 nm for 1 h shows essentially complete cleavage of SC DNA to its NC form (lanes 7 and 8). The DNA photocleavage activity of **2** and **3** could be due to the photosensitizing effect of the quinoxaline and phenazine moieties of the dpq and dppz ligands, respectively. Control experiments with only SC DNA exposed to 365 nm or SC DNA in the presence of dpq and dppz complexes in dark do not show any DNA cleavage activity. The ligands alone are cleavage inactive under similar reaction conditions. The DNA groove binding property of the complexes was studied using the DNA minor groove binder distamycin-A (Figure 4). Distamycin-A (50 μM) alone shows ~12% (lane 9) cleavage of SC DNA (30 μM) to its NC form at 365 nm on 1 h photo-exposure. Addition of the dpq complex to distamycin-A bound SC DNA causes significant inhibition in the photo-cleavage activity (lane 10). The dppz complex, however, displays no apparent inhibition (lane 11) suggesting minor and major groove binding preferences of the dpq and dppz complexes, respectively.[74]

The photo-induced DNA cleavage activity of the complexes in red light has been studied using a continuous-wave (CW) Ar−Kr mixed-gas ion laser with an IR attachment (752.5−799.3 nm optics) (Figure 5). We have chosen this wavelength considering the presence of a d-d band near 740 nm in the electronic spectra of the complexes. The phen complex as expected does not show any DNA cleavage activity (lane 6). The dpq and dppz complexes display significant cleavage of SC DNA to its NC form in red light (lanes 7 and 8). Unlike the organic dyes in PDT cleaving DNA by singlet oxygen pathway, photoexcitation of **2** and **3** seems to be metal-assisted involving the weak d-d band and photoactive ligand moieties resulting in an excited state that could generate different DNA cleavage-active species. Although there are some earlier reports on vanadium(V) complexes showing photocleavage of DNA in UV light, observation of DNA cleavage in near-IR light is rare in the literature.[46−50] Vanadyl(V) complexes of *N*-salicylidene amino acids are known to cleave plasmid DNA in UV light of $\lambda > 315$ nm.[50] Vanadyl(V)-peroxo complexes containing phenanthroline bases show DNA cleavage at 365 nm involving singlet oxygen species.[48] Bis(peroxo)vanadium(V) phenanthroline complexes and *N*-salicylidene-based vanadyl(V) complexes cleave DNA in UV light via formation of hydroxyl radicals.[49] We have recently reported the visible light-induced DNA cleavage activity of ternary oxovanadium(IV) complexes $[VO(L^1)(dppz)]$ having tridentate ancillary ligand (L^1), namely, *N*-salicylidene-*S*-methyldithiocarbazate (salmdtc) and *N*-salicylidene-L-methionate (salmet).[52,53] It has been observed that the salmdtc complex is a poor photocleaver of DNA in red light.[53] The salmet complex shows only moderate DNA photocleavage activity.[52] A comparison of the photo-induced DNA cleavage activity of the oxovanadium(IV) complexes reveals that complex **3** is a significantly better photocleaver of DNA in red light than its analogues (Figure 6 (a)).

Mechanistic Studies. The mechanistic aspects of the photo-induced DNA cleavage reactions of the complexes have been studied in the presence of different additives in UV-A and near-IR light (Figure 6 (b)). The complexes are cleavage inactive in UV-A light of 365 nm under argon atmosphere indicating the necessity of reactive oxygen species (ROS) for the DNA cleavage. The DNA cleavage reaction involving molecular oxygen could follow two major mechanistic pathways, namely, the type-II process forming singlet oxygen species or a photoredox pathway forming reactive hydroxyl radicals.[18] Addition of singlet oxygen quenchers like sodium azide, TEMP, or DABCO

(79) Otieno, T.; Bond, M. R.; Mokry, L. M.; Walter, R. B.; Carrano, C. J. *Chem. Commun.* **1996**, 37.

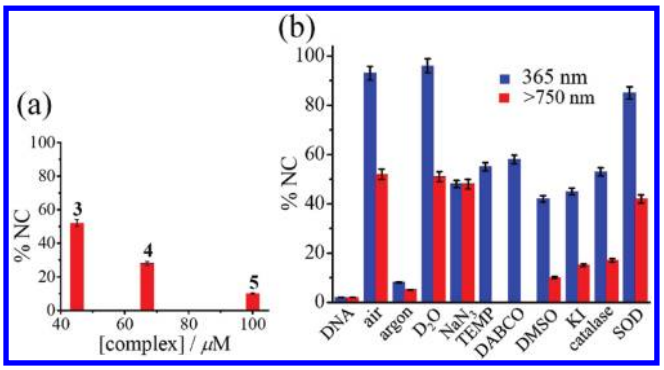

Figure 6. (a) Comparison of the DNA photocleavage activity of the oxovanadium(IV) complexes $[VO(L)(dppz)]Cl_2$ (**3**), [VO(salmet)(dppz)] (**4**), and [VO(salmdtc)(dppz)] (**5**) in red light of >750 nm for 2 h exposure time (salmet, *N*-salicylidene-L-methionate; salmdtc, *N*-salicylidene-*S*-methyldithiocarbazate; vide references 52 and 53 for complexes **4** and **5**). (b) Cleavage of SC pUC19 DNA (0.2 μg, 30 μM) by $[VO(L)(dppz)]Cl_2$ (**3**) in the presence of various additives in Tris-HCl buffer containing 1.5% DMF. The complex concentration and exposure time for 365 nm (blue light) experiments are 10 μM and 1 h, respectively. The complex concentration and exposure time for >750 nm (red light) experiments are 45 μM and 2 h, respectively. The additive concentrations/quantity are as follows: sodium azide, 0.2 mM; TEMP, 0.2 mM; DABCO, 0.2 mM; D_2O, 16 μL; DMSO, 4 μL; catalase, 4 units; and SOD, 4 units.

to SC DNA significantly inhibits the photo-induced DNA cleavage activity in UV-A light of 365 nm. Hydroxyl radical scavengers like DMSO or catalase also show partial inhibition in the DNA cleavage at this wavelength. The results suggest the involvement of both singlet oxygen ($^1O_2$) and hydroxyl radical ($^{\bullet}OH$) species at 365 nm. The formation of singlet oxygen is also evidenced from the reaction in D_2O showing enhancement of the cleavage activity because of longer lifetime of $^1O_2$ in this medium.[80] Vanadium(III) chloride, dpq and dppz do not show DNA cleavage activity at 365 nm under similar experimental conditions.

The photo-induced DNA cleavage reactions in the presence of additives are also studied at near-IR wavelength of >700 nm. Singlet oxygen quenchers show no inhibitory effect in red light. The hydroxyl radical scavengers, however, show inhibition in the DNA cleavage activity suggesting hydroxyl radical pathway in a photoredox reaction. The photoexcited vanadyl(IV) species in red light could reduce the metal forming reactive V(III) species that could lead to the formation of hydroxyl radicals following a Fenton-like mechanism known for iron-bleomycins and copper-dipyridoquinoxaline species.[21,81]

Protein Cleavage Activity. We have investigated the UV-A (365 nm) light-induced protein cleavage activity of the complexes **1**−**3** using 5 μM BSA and 10 μM lysozyme in Tris-HCl buffer containing 1.8% DMF by SDS-PAGE (Figure 7, Figure S13 in the Supporting Information). At respective complex concentrations of 125 μM and 100 μM, the dppz complex **3** shows complete degradation of BSA and the intracellular protein lysozyme. Although complexes are known to show photocleavage of proteins in site-specific manner, complex **3**

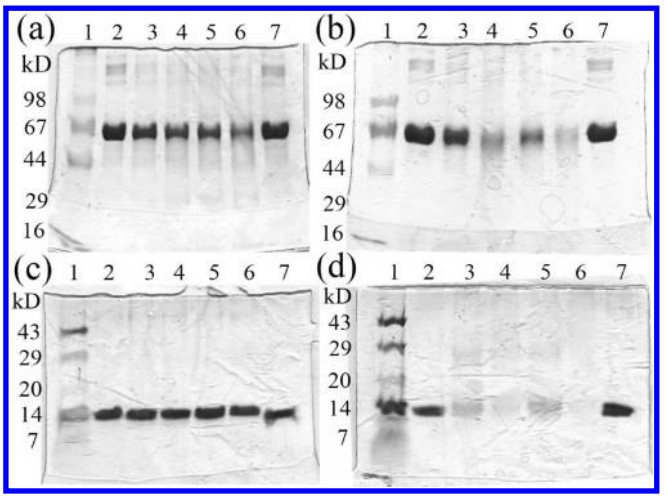

Figure 7. Photo-induced cleavage of bovine serum albumin (BSA, 5 μM) and lysozyme (10 μM) in UV-A light of 365 nm by the complexes $[VO(L)(B)]Cl_2$ (B: dpq, **2**; dppz, **3**) in 50 mM Tris-HCl buffer having 0.75% DMF (pH 7.2). Panels (a) and (b) represent complexes **2** and **3**, respectively, in 12.5% SDS-PAGE: lane 1, molecular marker; lane 2, BSA control; lane 3, BSA + complex (100 μM, 30 min.); lane 4, BSA + complex (100 μM, 1 h); lane 5, BSA + complex (125 μM, 30 min.); lane 6, BSA + complex (125 μM, 1 h); lane 7, BSA + complex (125 μM, in dark). Panels (c) and (d) represent complexes **2** and **3**, respectively, in 16.5% tricine-SDS-PAGE: lane 1, molecular marker; lane 2, lysozyme control; lane 3, lysozyme + complex (50 μM, 30 min.); lane 4, lysozyme + complex (50 μM, 1 h); lane 5, lysozyme + complex (100 μM, 30 min.); lane 6, lysozyme + complex (100 μM, 1 h); lane 7, lysozyme + complex (100 μM, in dark).

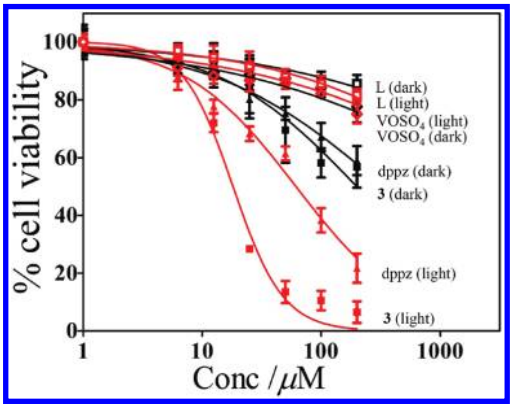

Figure 8. Photocytotoxicity of the dppz complex **3** along with the controls in non-small cell lung carcinoma (A549) on 3 h incubation in dark followed by photo-irradiation to visible light (400 to 700 nm) as determined by MTT assay. The dark-treated and photoexposed cells are shown by black and red symbols, respectively.

photocleaves proteins in non-specific manner.[82,83] Complex **3** does not show any protein cleavage activity in dark thus ruling out any hydrolytic protein damage. The MALDI mass spectrum of complex **3** in the presence of BSA in dark shows only the mass peak of BSA. This mass peak is found to be absent after the sample is irradiated with UV-A light of 365 nm suggesting complete degradation of the BSA protein (Figures S14, S15 in the Supporting Information). Control experiment with only BSA exposed to UV-A light under similar reaction conditions

(80) (a) Khan, A. U. *J. Phys. Chem.* **1976**, *80*, 2219. (b) Merkel, P. B.; Kearns, D. R. *J. Am. Chem. Soc.* **1972**, *94*, 1029.
(81) (a) Umezawa, H. *Prog. Biochem. Pharmacol.* **1976**, *11*, 18. (b) Burger, R. M. *Chem. Rev.* **1998**, *98*, 1153. (c) Wolkenberg, S. E.; Boger, D. L. *Chem. Rev.* **2002**, *102*, 2477.
(82) (a) Thota, J.; Kalpanie, B.; Kumar, C. V. *Photochem. Photobiol. Sci.* **2008**, *7*, 1531. (b) Kumar, C. V.; Thota, J. *Inorg. Chem.* **2005**, *44*, 825. (c) Cremo, C. R.; Loo, J. A.; Edmonds, C. G.; Hatlelid, K. M. *Biochemistry* **1992**, *31*, 491.
(83) Tanimoto, S.; Matsumura, S.; Toshima, K. *Chem. Commun.* **2008**, 3678.

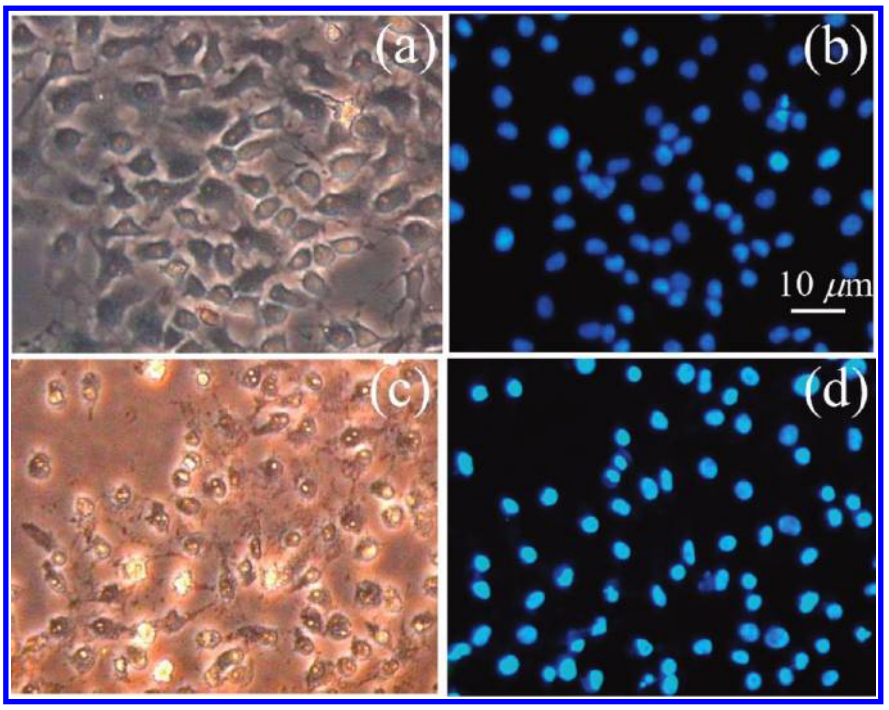

Figure 9. DAPI staining of nuclei of A549 cells (4 h post photoexposure) treated with complex **3** and visible light: (a) and (b) are the untreated control cells; (c) and (d) are the cells treated with 25 μM of **3**. Panels (b) and (d) were from a fluorescence microscope with 360/40 nm excitation filter and 460/50 nm emission filter. Panels (a) and (c) are the respective bright-field images of (b) and (d).

does not show any degradation of the protein. Complexes **1** and **2** are found to be inactive in cleaving BSA in UV-A light. The involvement of reactive oxygen species (ROS) in the cleavage reaction has been evidenced from mechanistic studies in the presence of additives like singlet oxygen quenchers NaN_3 (3 mM) and TEMP (3 mM) and hydroxyl radical scavengers DMSO (20 μL) and KI (3 mM) (Figure S17 in the Supporting Information). We have done mechanistic studies of protein cleavage in the presence of hydroxyl radical scavenger, namely, KI at different concentrations. The extent of inhibition is shown in Figure S16 (vide Supporting Information). It is observed that 3 mM KI leads to complete inhibition of cleavage. Both NaN_3 and TEMP do not show any apparent effect on photo-induced protein cleavage activity of **3** thus excluding the possibility of $^1O_2$ cleavage pathway. DMSO and KI additions cause significant reduction in the protein photocleavage activity suggesting the involvement of hydroxyl radicals as the reactive species (Figure S17 in the Supporting Information).

Cell Cytotoxicity and Nuclear Staining. Cellular photocytotoxicity of complex **3**, ligands and the metal salt has been studied on non-small cell lung carcinoma (A549) using MTT assay. The dppz complex **3** upon incubation for 3 h in dark followed by photoexposure with visible light (400−700 nm, 10 J cm^{-2}) shows a dose-dependent decrease in cell viability with an IC_{50} value of 17.03 μM (Figure 8). The IC_{50} value obtained from cells unexposed to light is 175 μM. Hence, a 10-fold enhancement in cell cytotoxicity is observed upon photoexcitation in visible light. In contrast, cisplatin, the most commonly used chemotherapeutic drug, is much less effective in A549 cells with an IC_{50} value of 64 μM.[84] Although Photofrin under similar conditions (halogen lamp, 10 J cm^{-2}) is known to give an IC_{50} value of 0.35 μM, the drug has undesirable toxic effects.[85] The dppz ligand alone is non-toxic in dark with an IC_{50} value >200 μM, but it shows photocytotoxicity giving an IC_{50} value of 61.14 μM in A549 cells (Figure 8). Ligand L and vanadyl sulfate as the metal salt are both non-toxic in dark and light giving a high IC_{50} value of >200 μM. The presence of oxovanadium(IV) moiety in complex **3** has significantly enhanced the PDT effect of the dppz ligand in visible light.

To determine the nuclear features and to gain insight into the pathway of cell death, we have carried out DAPI staining following PDT with complex **3** (Figure 9). The control cells permeabilized with detergent (0.1% Triton-X) exhibit light and evenly stained contours of the nuclei in contrast to the treated cells that show typical characteristics of cells undergoing apoptosis (Figure 9(b)). The treated cells are seen to possess fragmented or highly condensed nuclei while the bright field images provide evidence for cell shrinkage and membrane blebbing attributed to the typical features of apoptotic cells (Figure 9(d)). Necrotic nuclei are not observed with DAPI staining. The DAPI staining indicates apoptotic mode of cell death following PDT with complex **3**.

Conclusions

In summary, we present the photo-induced DNA and protein cleavage activity of a new class of oxovanadium(IV) complexes in UV-A and near-IR visible light. The photocytotoxic property of the dipyridophenazine complex in visible light is reported. The $3d^1$-VO^{2+} complexes of

(84) Zhang, P.; Gao, W. Y.; Turner, S.; Ducatman, B. S. *Molecular Cancer* **2003**, *2*, 1.

(85) Nishiyama, N.; Nakagishi, Y.; Morimoto, Y.; Lai, P.-S.; Miyazaki, K.; Urano, K.; Horie, S.; Kumagai, M.; Fukushima, S.; Cheng, Y.; Jang, W.-D.; Kikuchi, M.; Kataoka, K. *J. Controlled Release* **2009**, *133*, 245.

phenanthroline bases having VON_5 coordination geometry show DNA binding propensities. The dpq and dppz complexes are efficient photocleavers of DNA in UV-A light of 365 nm following both singlet oxygen and hydroxyl radical pathways. Both the complexes display significant DNA cleavage activity in near-IR light of >750 nm by hydroxyl radical pathway. Unlike copper(II) complexes of planar phenanthroline bases that are known to be efficient chemical nucleases, the present oxovanadium(IV) complexes show poor chemical nuclease activity. The DNA cleavage observed on photoactivation of the oxovanadium(IV) complexes at a near IR wavelength is of significance since compounds showing photo-induced DNA cleavage at near IR light are rare in the literature. Among the macrocyclic organic dyes, only lutetium texaphyrin (LUTRIN) is known to show PDT effect at such a long wavelength (λ_{max}, 732 nm).[1,3] The dppz complex shows photocleavage of intracellular protein lysozyme. This observation is important for developing metal-based anti-metastasis agents to control tumor malignancy using light. The observation of low dark cytotoxicity and significant photocytotoxicity of the dppz complex **3** in visible light in non-small cell lung carcinoma/human lung adenocarcinoma A549 cells is of importance toward designing and developing oxovanadium(IV) complexes as potential agents for cellular applications in PDT.

Acknowledgment. We thank the Department of Science and Technology, Government of India, for the financial support (SR/S5/MBD-02/2007) and the CCD diffractometer facility. S.S. thanks the Council of Scientific and Industrial Research, New Delhi, for a fellowship. We are grateful to the Alexander von Humboldt Foundation, Germany, for an electrochemical system. A.R.C. thanks the DST for the J. C. Bose national fellowship.

Supporting Information Available: Crystallographic details in CIF format for complex **1**, ESI-MS spectra, cyclic voltammograms, unit cell packing diagram, DNA binding, DNA and protein photocleavage data (Figures S1−S17). This material is available free of charge via the Internet at http://pubs.acs.org.